Contents lists available at ScienceDirect

Neurocomputing

journal homepage: www.elsevier.com/locate/neucom

Ultrasonic signal classification and imaging system for composite materials via deep convolutional neural networks

Min Meng [a,b,*], Yiting Jacqueline Chua [b], Erwin Wouterson [b], Chin Peng Kelvin Ong [b]

[a] Department of Computer Science, Guangdong University of Technology, Guangzhou, China
[b] School of Mechanical and Aeronautical Engineering, Singapore Polytechnic, Singapore

ARTICLE INFO

ABSTRACT

Automated ultrasonic signal classification systems are finding increasing use in many applications for the recognition of large volumes of inspection signals. Wavelet transform is a well-known signal processing technique in fault signal diagnosis system. Most of the proposed approaches have mainly used low-level handcraft features based on wavelet transform to encode the information for different defect classes. In this paper, we proposed a deep learning based framework to classify ultrasonic signals from carbon fiber reinforced polymer (CFRP) specimens with void and delamination. In our proposed algorithm, deep Convolutional Neural Networks (CNNs) are used to learn a compact and effective representation for each signal from wavelet coefficients. To yield superior results, we proposed to use a linear SVM top layer in the training process of signal classification task. The experimental results demonstrated the excellent performance of our proposed algorithm against the classical classifier with manually generated attributes. In addition, a post processing scheme is developed to interpret the classifier outputs with a C-scan imaging process and visualize the locations of defects using a 3D model representation.

© 2017 Published by Elsevier B.V.

1. Introduction

Ultrasonic methods are the most successful non-destructive testing (NDT) technique for quality assessment and detection of flaws in engineering materials and the pulse-echo is the most commonly used for its simplicity and efficiency [1]. In this technique, a piezoelectric ultrasonic transducer is used to generate ultrasonic waves which propagate through metal plate. Thus, they are reflected by defect and return back to transducer surface. The same ultrasonic transducer receives the reflected waves and converts them to electrical signals. These signals, called A-scan signals, contain information about the type, size and orientation of the defect [2].

The identification of defects on A-scan signal is not a trivial task and usually called *ultrasonic pattern recognition* [3]. The results usually depend on the experience and knowledge of the experts. To minimize errors due to human subjectivity, automatic signal classification system (ASCS) is becoming increasing important and has the advantage of detecting flaws and interpreting ultrasonic signals consistently and accurately [4]. Some researchers [2,3,5,6] define three major tasks to such systems: preprocessing raw data, fea-

ture extraction and classification. The preprocessing task normalizes the raw data signals values to a suitable range for other tasks. The feature extraction task is responsible to obtain attributes from normalized A-scan signals. The obtained attributes must be able to characterize the flaws. Finally the classification task aims to analyze the attributes from an A-scan signal and indicates one from a known set of flaws. The algorithm that implements a classification task is called *classifier*. Several approaches have been proposed to build a classifier, such as traditional statistical classifiers, rule-base classifiers and learning-base classifiers [7], which typical examples are artificial neural network (ANN) [8,9] and support vector machine (SVM) [10–12].

As one of the most important techniques, feature extraction will directly affect the accuracy and reliability of signal classification. Deep learning using neural networks develop rapidly recently and have achieved success in a wide range of tasks. We propose to use deep learning to extract powerful representations from the input signals. Instead of low-level handcraft features, we train Convolutional Neural Networks (CNNs) to get high-level features to improve the performance for signal classification. Wavelet transformation can divide the signal gradually in multi-scale by means of dilation and translation. Inspired by [13], the wavelet transform coefficients are re-organized into a 2D feature matrix which is taken as the input to the CNNs to facilitate the training process and utilize the convolutional characteristics of CNNs. The deep CNNs are

* Corresponding author at: School of Mechanical and Aeronautical Engineering, Singapore Polytechnic, Singapore.
  E-mail address: mengmin1985@gmail.com (M. Meng).
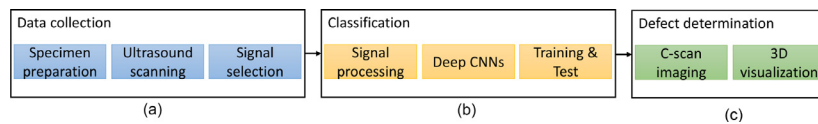
Fig. 1. Flowchart of our proposed approach. (a) Data collection including specimen preparation, ultrasound scanning and signal selection is carried out during the experimental procedure; (b) Signal classification tasks are completed through signal processing, deep architecture construction and training/testing. (c) Defect determination is performed through C-scan imaging and 3D visualization representation.

devoted to learn a compact and effective representation for each signal from wavelet coefficients in our framework. In this manner, the proposed deep CNNs are trained as a multi-class classifier to predict the class of the input signals.

As an alternative to softmax, support vector machine (SVM) is widely used for classification. In [14], the L2-SVM objective was used for the output layer of a deep Convolutional Neural Network to obtain more discrimination power of classification. This kind of output layer for classification using the hinge loss as cost function is also proposed in [15] to make comparison with the commonly applied softmax. Smoother learning curve and slightly increased accuracy are obtained when using this objective in our deep architecture. Thus a linear SVM top layer instead of softmax is proposed to train the networks to yield superior results for signal classification task.

For defect determination, it is usually beneficial to obtain a two-dimensional representation through a C-scan imaging process [16]. Other than the C-scan image obtained purely depending on the signal amplitude, we propose a post processing scheme to compute the C-scan image which takes the classifier outputs as input and further create the three-dimensional (3D) model representation to visualize the locations of defects. To our knowledge, it is the first attempt to present the defects in 3D view which provides new potential ways to localize and characterize the defect for ultrasound testing in the future.

This work conducts a study on ultrasonic signals very similar to each other obtained from artificial inserts in a carbon fiber reinforced polymer (CFRP) plate. First, a process was developed to produce CFRP laminates and artificial defects with void, delamination were collected for our experiments. Then we present an automated signal classification system based on the deep convolutional neural networks to process A-scan signals acquired with the ultrasound transducer. To complement the system, an additional post processing is developed to interpret the classification results with a C-scan imaging process and visualize the locations of defects using a 3D model representation. The flowchart of our proposed approach is shown in Fig. 1.

1.1. Contributions

The main contribution of this work is three-fold:

- A deep learning based framework is proposed to classify ultrasonic signals from carbon fiber reinforced polymer specimens in an automated signal classification system.
- A linear SVM top layer is used in the training process of signal classification task to yield superior results.
- A post-processing scheme is developed to interpret the classifier outputs and present the defects in 3D view.

1.2. Related work

In the last years, various efforts have been made in devising an automated signal classifications system such that we restrict the discussion to the most important aspects including feature selection techniques and classification algorithms.

Simone et al. [9] presented serval techniques including discrete Gabor transform, discrete wavelet transform (DWT) and clustered DWT methods for ultrasonic signals classification. ANN are trained based on the these features and the results demonstrated the effectiveness of the clustered DWT method for feature extraction. Matz et al. [10] used the DWT based method for filtering of ultrasonic signal in combination with SVM to automatically classify ultrasonic signals of in the form of different fault echoes. Cacciola et al. [11] proposed an heuristic approaches based on the use of DWT and PCA in feature extraction and selection. The SVM classifier trained on these features has good performance for classifying the ultrasonic echoes measured on defective CFRP specimen. Wang [5] utilized the DWT and wavelet packet transform (WPT) for feature extraction. ANNs and SVMs are trained to validate the effectiveness of different wavelet transform based features for classifying the ultrasonic flaw signals from CFRP specimens. Like most of the methods mentioned above, we adopted wavelet transform based methods for feature extraction in this paper due to the non-stationary characteristics of ultrasonic flaw signals.

For the classification purposes, the classifiers of choices are mainly learning-based classifier, which typical examples are ANN and SVM. recently as a subfield of machine learning, deep learning have been widely applied in traditional artificial intelligence domains such as natural language processing [17], transfer learning [18] and computer vision [19–21] and many more. we refer the reader to a recent more complete survey [22]. Hong et al. [23,24] proposed hypergraph regularized autoencoder for feature extraction with deep learning for image-based human pose recovery. Yu et al. [25] developed a deep multi-modal distance metric learning method based on the click and visual features for image ranking. It is worth noting that A-scan signals are very similar to each other and only have subtle variances that are very difficult to classify. In our study, we first attempt to use deep learning to process A-scan signals for ultrasonic flaw classification.

1.3. Outline

This paper is organized as follows. Section 2 gives a brief introduction to the wavelet transform. Section 3 demonstrates the experimental procedure. The deep learning architectures are described in Section 4. Experimental results are presented in Section 5. Section 6 introduces a post processing algorithm to localize and characterize defect information followed by conclusions in Section 7.

2. Wavelet transform

The wavelet transform is a windowing technique with variable-sized regions, which allows the use of long time intervals to obtain more precise low frequency information and shorter regions where high frequency information is required [26]. The structure of wavelet packet transform (WPT) is similar to discrete wavelet transform (DWT) [27]. The main difference in these two techniques is, the WPT can simultaneously break up detail and approximation versions but DWT only breaks up as an approximation version. Therefore, the WPT have the same frequency bandwidths in each resolution and DWT does not have this property. The WPT suits signal processing, especially non stationary signals because the same frequency bandwidths can provide good resolution
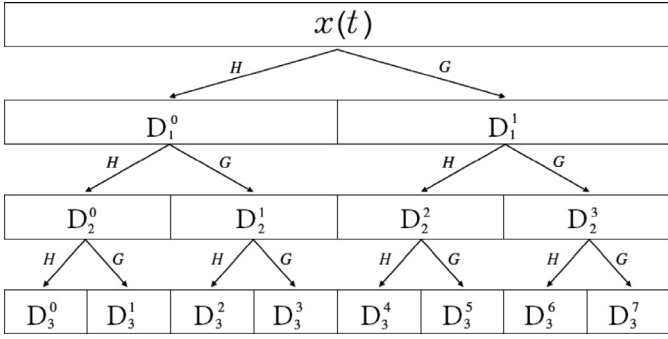
Fig. 2. Tree structures of wavelet packet transform.

regardless of high and low frequencies. The principle of WPT is described as follows [28–30].

The wavelet packet function can be defined as

$$W_{j,k}^n(t) = 2^{\frac{j}{2}} W^n(2^j t - k), \tag{1}$$

where j and k are the index of scale and translation operations and n is an operation modulation parameter or oscillation parameter. The first two wavelet packet functions are the scaling and mother wavelet functions: $W_{0,0}^0(t) = \phi(t), W_{0,0}^1(t) = \psi(t)$. When $n = 2, 3, \cdots$, the functions can be defined recursively by the relationship:

$$W_{0,0}^{2n}(t) = \sqrt{2} \sum_k h(k) W_{1,k}^n(2t - k),$$

$$W_{0,0}^{2n+1}(t) = \sqrt{2} \sum_k g(k) W_{1,k}^n(2t - k), \tag{2}$$

where $h(.)$ and $g(.)$ are the half-band low-pass and high-pass filter associated with the predefined scaling function and mother wavelet function. The coefficients resulting from the decomposition of a signal $x(t)$ can be computed as

$$d_{j,k}^n = \langle x(t), W_{j,k}^n(t) \rangle. \tag{3}$$

The framework of WPT algorithm broken up to three resolution levels for signal $x(t)$ is shown in Fig. 2. In the figure, D_j^n represents the symbol for a subspace that stands for the jth resolution and the nth subspace. In the present study, the ultrasonic signals will be broken up to the fourth level $j = 4$ and Daubechies's wavelet of order 5 is used for filtering. As a result, sixteen subspaces ($2^j = 2^4 = 16$) will be produced for four resolutions and wavelet frequency intervals of each subspace can be computed by

$$((n - 1)2^{-j-1} f_s, n2^{-j-1} f_s], n = 1, 2, \cdots, 16, \tag{4}$$

where f_s is sampling frequency.

3. Experimental procedure

3.1. Specimen preparation

Carbon fibers are increasingly used in the aerospace and automotive industries. Common techniques adopted to manufacture composite structures include conventional hand lay-up method, resin infusion and recently there is a shift toward (tailored) fiber placement and tape laying. All these methods aim to produce composite laminates of good quality with minimum amount of defects, i.e. dry spots, causing delamination in the structures [31,32], which could eventually lead to failure. Besides delamination, voids and micro-cracks are commonly found in defects in composite structures.

A process was developed to produce carbon fiber reinforced plastics (CFRP) with minimum amount of defects. TORAY 12K
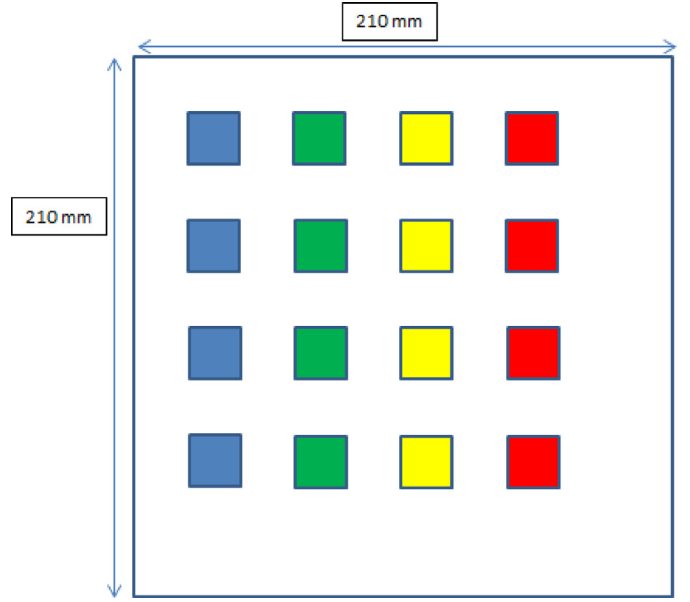

Fig. 3. Locations of the delamination defects in CFRP laminate at various depths, i.e. 3rd, 6th, 9th and 12the layer. Four defects of 20mm in size are placed at each depth by the column, depth in turn deepened from right to left. (For interpretation of the references to colour in this figure legend, the reader is referred to the web version of this article.)

twill weave carbon fiber fabrics were cut to a length of 310mm and a width of 310mm. Fifteen layers of carbon fabrics were impregnated with two part epoxy resin, Epikote 1006A using hand lay-up method. The layers were placed in between two glass molds to give smooth surfaces, enhancing ultrasonic scanning. The layup was cured under vacuum at room temperature for 24 h. The average thickness of the CFRP laminates was measured to be 3.6mm. A water-jet cutter was used to cut the laminates to a length of 210mm and a width of 210mm for NDT measurements.

A similar process was used to produce the CFRP laminates with defects. The type, position and size of each inserted defects were recorded during the fabrication process. Fig. 3 shows a sample containing delamination defects of 20mm in size, placed at different depths (i.e. 3rd, 6th, 9th and 12th layer).

3.2. Signal acquisition and selection

Olympus Omniscan MX2 was used to scan composite structures for defects. For the CFRP laminates, a 5 MHz near-wall probe with 64 elements and a wedge (SNW1-0L-AQ25) were used. In order to reduce the noise signals, the CFRP laminates were submerged in water. The A-scan signal was digitized at a sample length of 512.

In this study, the inspection was performed on 10 specimens of CFRP laminates and artificial defects with void, delamination were collected for our experiments. The database was created consisting of a total number of 6,000 ultrasonic A-scan signals which were equally divided into the 12 classes: ten delamination classes with layer number 3–7 and 9–13, one void class and one class of signals showing absence of defect. It is noteworthy that, A-scans from delamination defects of neighboring layers are very similar to each other and only have subtle variances that are very difficult to classify using the manually generated attributes from normalized signals.
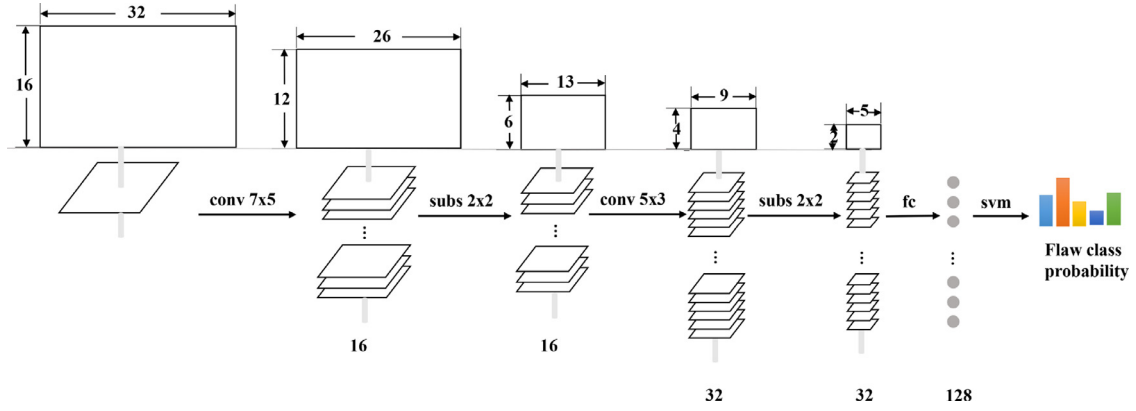
Fig. 4. Architecture of the proposed deep CNNs. Here conv, subs, fc stand for convolutional, sub-sampling, fully-connected layers respectively.

4. Deep learning approach

In this section, the deep learning approach developed will be introduced.

4.1. Signal processing

After signal processing by using wavelet packet decomposition, the original time domain signal was transformed into the coefficients $d_{j,k}^n$. At four resolutions level, a time series signal with 512 sample points will have 16 subspaces with 32 samples per sub-band. These coefficients have a defined ordering and therefore can be thought of as information within the original signal in different frequency band. To facilitate the training process of CNNs similar to [13], we re-organize the coefficients into a 2D feature matrix with dimensions 32×16. Treating the wavelet transform coefficients in this way allows to utilize the capabilities of CNNs to get high-level features which combines signal information from all frequency intervals.

4.2. Structure of deep CNNs

Fig. 4 shows the structure of the deep CNNs in our proposed algorithm. As we can see, two convolutional layers, one fully connected layers and one output layer are contained in the deep learning architecture.

In the first convolutional layer, sixteen 7×5 kernel filters are applied to the input coefficient matrix. After the convolution, a non-linearity module with a sigmoid activation function $(i.e. sigmoid(x) = (1 + exp(-x))^{-1})$ is applied to generate the feature maps. We down-sample the feature maps by a factor of 2 for each dimension to generate sixteen 6×13 feature maps.

In the second convolutional layer, we generate 32 new feature maps by applying 5×3 kernel filters to the input feature maps obtained above. The non-linearity mapping followed by subsampling are carried out to generate 32 down-sampled 2×5 feature maps. In this manner, the coefficients can be non-linearly combined and hierarchically compressed through various convolutional operations in the proposed networks.

4.3. Loss function of signal classification

For classification problems using deep learning techniques, the standard choice for the activation function at the top layer of a network is the *softmax* function defined by

$$softmax(x_i) = \frac{e^{x_i}}{\sum_j e^{x_j}} \tag{5}$$

with x_i and x_j being the value of dimension i and j of a vector $\mathbf{x}$. The $softmax(x_i)$ specifies a discrete probability distribution and sum up to one by definition. Instead of minimizing the cross-entropy or maximizing the log-likelihood by *softmax* function, the L2-SVM training objective given by

$$\min_x \frac{1}{2} w^T w + C \sum_n \max(0, 1 - y_n (w^T x_n + b))^2 \tag{6}$$

is proposed in [14]. Every output neuron is treated as a linear SVM in this approach. In this way, the output layer of the network becomes a multi-class SVM-predictor, which is trying to find the maximum margin between signal points of different classes. The main difference to a normal linear multi-class SVM-predictor is that, the inputs to the SVMs are heavily transformed by previous layers of the network. In this paper, we use L2-SVM's objective as the loss function to train deep CNNs for signal classification.

4.4. Manually generated features

To investigate how well deep CNNs would perform on hand-crafted features, we also implement two exemplary ways of hand-crafting features for comparison.

Statistical parameters: A feature vector S of eight informative features were extracted from the WPT coefficients representation of each signal [5]:

1. Mean value: $M = \frac{1}{N} \sum_{i=1}^N x_i$
2. Standard deviation: $V = \sqrt{\frac{1}{N-1} \sum_{i=1}^N (x_i - m)^2}$
3. Maximum amplitude: $Max = \max_{1 \leq i \leq N} (x_i)$
4. Minimum amplitude: $Min = \min_{1 \leq i \leq N} (x_i)$
5. Maximum energy: $\max^2(|Max|, |Min|)$
6. Average frequency
7. Frequency of minimum energy samples
8. Half point (HaPo): the frequency that divides up the spectrum into two parts of same area.

Shannon entropy: Entropy is a measure of uncertainty that is used in various fault conditions. For ultrasonic signals with different flaws, the entropy at given scales are always varied and can be considered as an important feature for classification. By using WPT decomposition, the wavelet entropy is applied to wavelet coefficients and can be calculated as [33]:

$$E_{j,i} = \sum_k d_{j,k}^{n2} log(d_{j,k}^{n2}), \tag{7}$$

where $d_{j,k}^n$ is the WPT coefficients of the subspace after wavelet packet decomposition. Let $E_{4,i} (i = 0, 1, \cdots, 15)$ denote

Table 1
Recognition rate of our proposed approach.

	Recognition rate (%)	
	Training data	Test data
Delamination (layer)		
3rd	99.67	98.34
4th	100	99.41
5th	99.86	99.17
6th	99.67	97.26
7th	99.69	95.75
9th	99.76	95.4
10th	100	97.73
11th	99.94	97.39
12th	100	98.75
13th	99.95	98.6
Void	100	100
Non defect	100	100
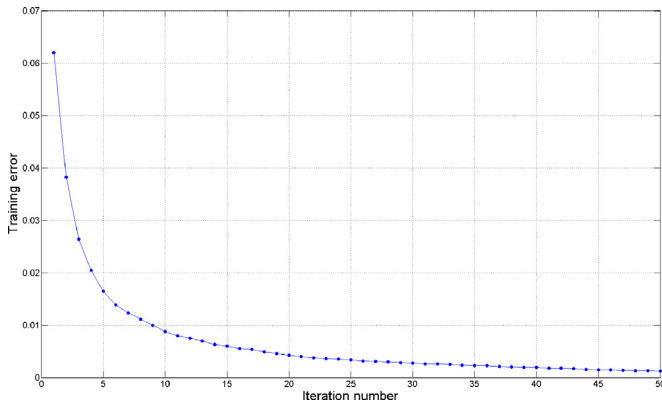
Fig. 5. Training error convergence curve. One iteration error is obtained by averaging the errors of all the training signals.

the sequence of the entropy of WPT decomposition at the fourth level, then a feature vector T can be expressed as $T = [E_{4,0}, E_{4,1}, \cdots, E_{4,14}, E_{4,15}]$.

5. Results and discussion

The performance of the proposed approach was tested on a test data set consisting of A-scan signals collected from ten specimens. As described in Section 3, the signals consist of 10 classes of delamination (3rd–7th layers and 9th–13th), one class of void and one class of signals presenting no defect. The number of experimental data is 6000 in total, consisting of 500 sets per class. The 5000 data sets are used to training and the rest 1000 data sets are used to test the recognition rate of the proposed network.

Table 1 summarized the recognition rate of the proposed approach. We can observed that the proposed approach produces consistent classification results. The recognition rates for all classes are consistently above 95%. Typically, A-scan signals from delamination defects of neighboring layers only have subtle variance in their echo peak positions that are very difficult to separate from each other. To overcome this problem, our method hierarchically combines the wavelet transform coefficients by learning a set of weights in different layers of CNNs. In this way, the coefficients can be non-linearly combined and hierarchically compressed through various convolutional operations in CNNs that can be used to effectively discriminate between different classes. Fig. 5 shows the convergency curve of the propose method. Our method can achieve convergency through a few of iterations.

To understand the effectiveness of the proposed system, various tests were performed to evaluate the overall approach in the choice of feature extraction and classifier's objective functions in

Table 2
Overall classification results for the proposed classifier with different feature extraction methods.

	Recognition rate (%)	
	Training data	Test data
Statistical parameters	95.22	86.34
Shannon entropy	97.57	92.55
CNNs	99.87	98.15

Table 3
Overall classification results for the proposed network using different loss functions at the top.

	Recognition rate (%)	
	Training data	Test data
softmax	98.51	97.06
L2-SVM	99.87	98.15

Table 4
Overall classification results for different classifiers by using the features represented by WPT coefficients.

	Recognition rate (%)	
	Training data	Test data
ANN	98.18	95.25
SVM	98.51	97.63
CNN	99.87	98.15

particular. Table 2 shows the overall classification results for the proposed classifier with different feature extraction methods. Compared with ours, the other two methods perform poorly for the classification results. The Shannon entropy is better than the statistical parameters. Obviously, the statistical and entropy features of WPT coefficients cannot effectively describe the characteristics of ultrasonic signals for different flaws because it is hard to select the features with the best discrimination power. The proposed network performs much better than hand-crafting features owing to its ability to learn powerful representation from input signals.

Table 3 shows a comparison of classification accuracies for the proposed network using different loss functions at the top. Overall the L2-SVM outperforms the *softmax* due to its higher generalization capability for classification problem. Therefore, the L2-SVM's objective provides a better classification and has been selected as the performing scheme for our classification task.

As described in Section 1.2, wavelet transform based methods are mostly adopted for feature extraction. For the purpose of comparison with the state-of-the-arts, we performed signals classification task with different learning-based classifiers using the features represented by WPT coefficients. Table 4 summarized the classification accuracies using our algorithm and the algorithm proposed in [5] where we chose the best feature extraction strategy for the two classifiers ANN and SVM. The experimental results show that, although all three classifiers achieved effectiveness in the recognition, however, the deep learning based classifier proposed in our approach outperforms the other two popular classifiers.

6. Post processing for defect determination

In this section, we developed a post processing scheme to localize and characterize defect information.

6.1. Representation of ultrasound signals

The ultrasonic signals can be represented in different ways for defect determination, as shown in Fig. 6. The A-scan shows the
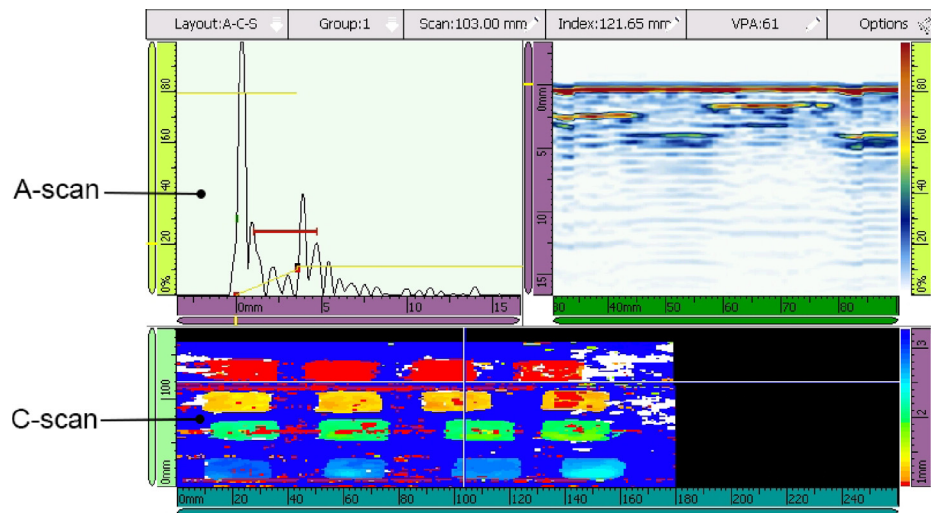
Fig. 6. Ultrasound signal representation.

amplitude of the signals acquired with ultrasound sensors. Despite A-scan is the common representation used in non-destructive testing, it is usually beneficial to obtain a two-dimensional representation through a C-scan imaging process for defect determination [16]. The C-scan shows the top view of the sample parallel to the scanning surface. By the means of integrating amplitudes of A-scan signals within a time range over the surface, the C-scan image is able to confirm the presence of a defect in the sample according to the changes in amplitude.

While moving the probe on the surface of the sample, it was observed that the A-scan signal kept varying in amplitude, suggesting it to be a good indicator for the presence of defects however maybe too sensitive to the random noise during the scanning procedure. This will influence the C-scan imaging process and the C-scan image purely depending on the amplitude is not reliable for defect determination. Thus a C-scan imaging process that relies on the signal classification is required to provide a high confidence of C-scan representation.

6.2. C-scan imaging process

Experiments on the proposed classifier have shown its performance in ultrasonic signal classification and can be utilized as the input to the C-scan imaging process to further characterize the detection area.

As an alternative for traditional C-scan imaging process, our C-scan image is produced according to the following steps:

- With the proposed classifier, A-scan signal is indicated as a known type of defect classes which are provided as input for the C-scan imaging of the sample
- For signal points in each defect class, a connect component labeling is performed on the C-scan image to further determine the defect area on the sample.
- We retain the points with neighbors belonging to the same class on the image and eliminate the others from C-scan image as random noise

Fig. 7 shows an example for the C-scan imaging process. Fig. 7a is naive C-scan image produced purely depending on the amplitude of raw A-scan signals. The different color-coding of the defects indicates the various depths at which the defects are located. Despite naive C-scan image roughly confirms the presence of the defects, the imaging process seems too sensitive to the amplitude change of A-scan signal and contains signal points which should be treated as random noise. Instead of traditional C-scan imaging
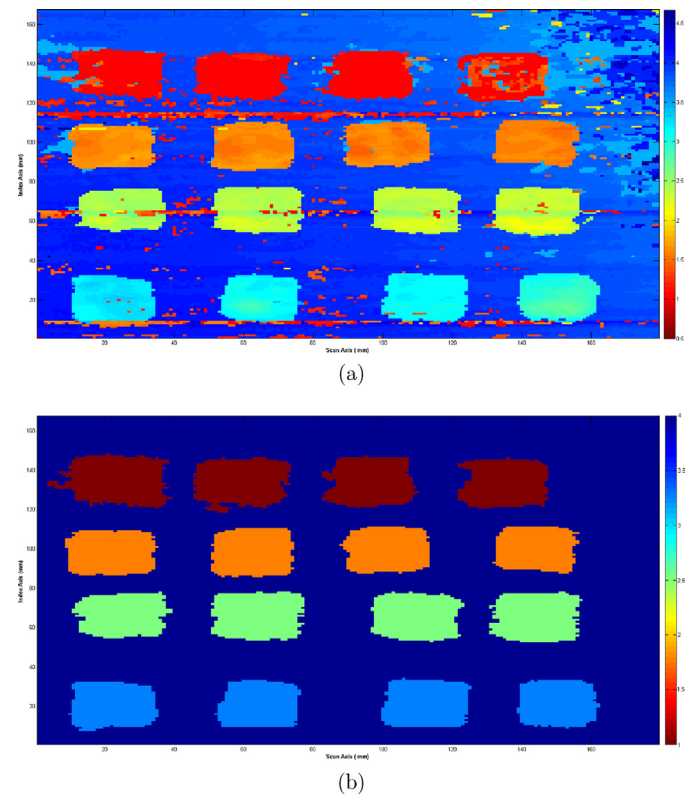

(a)

(b)

Fig. 7. C-scan imaging process based on the signal classification for CFRP laminates with defects at various depths. (a) naive C-scan image, (b) C-scan image produced with A-scan signal classification.

process, we utilize the classification of A-scan with the classifier to determine whether the signals indicated as defect in naive C-scan actually indicate the presence of a defect or not. Compared with the naive C-scan, we can provide a high confidence of C-scan representation to ensure the reliability of defect determination. In Fig. 7b, A-scan signal classification by the proposed classifier are used as input for the C-scan imaging process and the obtained C-scan image shows a clear view of defects parallel to the scanning surface, which are perfectly match with the defects placed during the fabrication of the specimen.

(a)

(b)
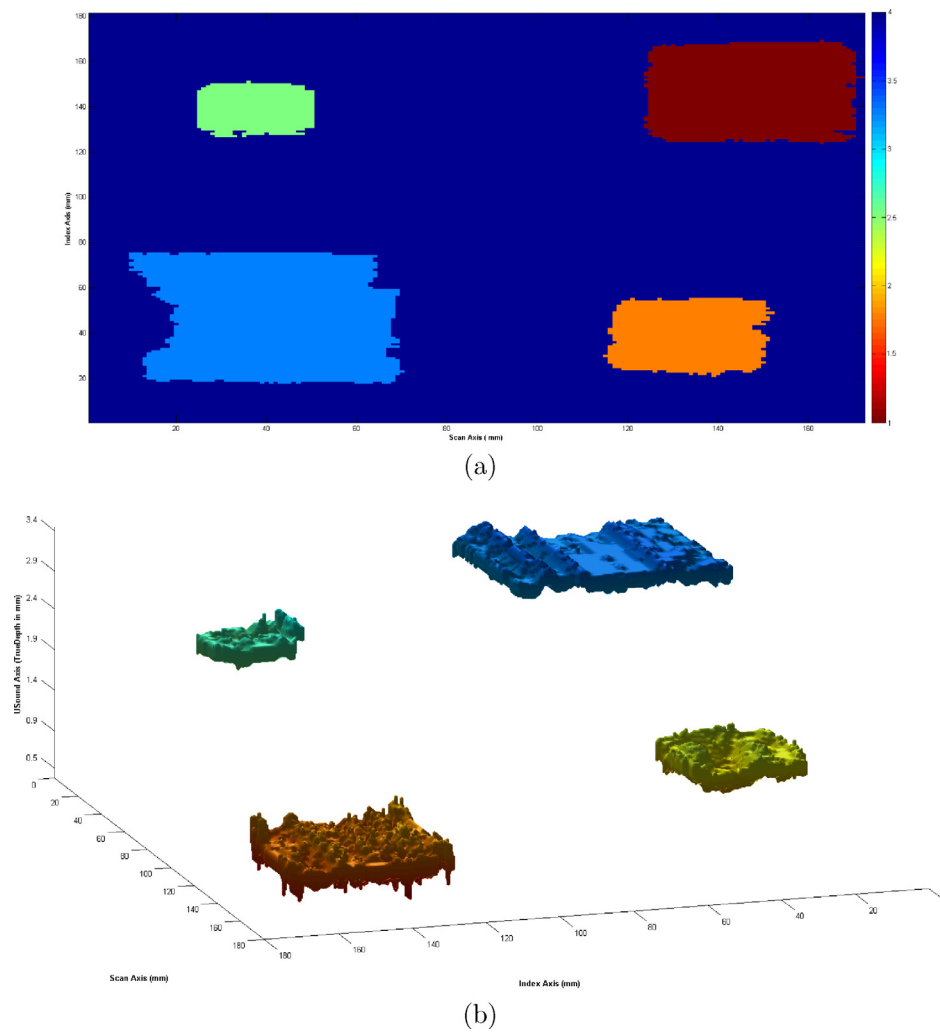
Fig. 8. 3D visualization of defects of various sizes at various depths for CFRP laminates. (a) C-scan image produced with A-scan signal classification, (b) a clear visualization of the defects in 3D representation model.

6.3. 3D visualization of defect

Although the C-scan representation confirms the presence of defects through showing a clear top view of the sample parallel to the scanning surface, it lacks the locations information of the defects. Thus it would be very helpful if we can visualize the locations of defects in 3D model representation. In this study, we further reconstruct the defects in 3D model showing a clear visualization of the locations of various defects.

The reconstruction of defects is described as follows:

- For signal point in each defect class, the location is indicated as the peak position of A-scan amplitude which is nearest to the layer location of the defect class it belongs to.
- According to the estimated locations, the 3D model representation is crated through a smooth surface fitting for each defect class.

Fig. 8 shows another example for CFRP laminates with defects of various sizes at various depths. All four defects of various size are visible in the C-scan image shown in Fig. 8a. However, we cannot see any differences or trends of the defect locations for signal points within each defect class from the top view of sample. To overcome this problem, the defects are reconstructed in 3D representation model showing a clear visualization of the lo-

cations of defects. A 3D model representation that displays the locations of various defects at various depths is shown in Fig. 8b. we can observe that, the 3D locations of defects are varied for signal points within the same defect class which maybe caused by the fabrication of the sample. Compared with the C-scan, 3D visualization of defects is capable of providing richer information for defect locations.

7. Conclusions

In this paper, we propose an automatic ultrasonic signal classification system using deep convolutional neural networks and signal processing techniques. A digital flaw detector is first used to acquire the signals of defective CFRP specimens with void and delamination. The networks are trained by signal classification task based on wavelet transform coefficients. Compared to the handcrated features, the network trained is capable of learning informative features that could discriminate the defect classes consistently. To further improve the classification rate, we use a deep linear SVM at the top layer to find the maximum margin between signals of different classes. In the classification, the experimental results show that the algorithm developed was effective in classifying the defect signals obtained through ultrasonic testing. For defect determination, a post processing scheme is de-

veloped to interpret the classifier outputs with a C-scan imaging process and visualize the locations of defects using a 3D model representation.

Acknowledgments

References

[1] J.L.B.C. Veiga, A.A.d. Carvalho, I.C.d. Silva, J.M.A. Rebello, The use of artificial neural network in the classification of pulse-echo and TOFD ultra-sonic signals, J. Braz. Soc. Mech. Sci. Eng. 27 (2005) 394–398.

[2] S. Sambath, P. Nagaraj, N. Selvakumar, Automatic defect classification in ultrasonic NDT using artificial intelligence, J. Nondestructive Eval. 30 (1) (2011) 20–28.

[3] S.-J. Song, H.-J. Kim, H. Cho, Development of an intelligent system for ultrasonic flaw classification in weldments, Nucl. Eng. Des. 212 (1) (2002) 307–320.

[4] S. Iyer, S.K. Sinha, B.R. Tittmann, M.K. Pedrick, Ultrasonic signal processing methods for detection of defects in concrete pipes, Autom. Construct. 22 (2012) 135–148.

[5] Y. Wang, Wavelet transform based feature extraction for ultrasonic flaw signal classification, J. Comput. 9 (3) (2014) 725–732.

[6] P.K. Wong, Z. Yang, C.M. Vong, J. Zhong, Real-time fault diagnosis for gas turbine generator systems using extreme learning machine, Neurocomputing 128 (2014) 249–257.

[7] J. Yu, Y. Rui, D. Tao, Click prediction for web image reranking using multimodal sparse coding, IEEE Trans. Image Process. 23 (5) (2014) 2019–2032.

[8] F.d.O. Saraiva, W.M. Bernardes, E.N. Asada, A framework for classification of non-linear loads in smart grids using artificial neural networks and multi-agent systems, Neurocomputing 170 (2015) 328–338.

[9] G. Simone, F. Morabito, R. Polikar, P. Ramuhalli, L. Udpa, S. Udpa, Feature extraction techniques for ultrasonic signal classification, Int. J. Appl. Electromagn. Mech. 15 (1–4) (2001) 291–294.

[10] V. Matz, M. Kreidl, R. Smid, Classification of ultrasonic signals, Int. J. Mater. Product Technol. 27 (3–4) (2006) 145–155.

[11] M. Cacciola, S. Calcagno, F.C. Morabito, M. Versaci, Computational intelligence aspects for defect classification in aeronautic composites by using ultrasonic pulses, IEEE Trans. Ultrasonics Ferroelectr. Frequency Control 55 (4) (2008) 870–878.

[12] Z. Yin, J. Hou, Recent advances on SVM based fault diagnosis and process monitoring in complicated industrial processes, Neurocomputing 174 (2016) 643–650.

[13] K. Guo, D. Zou, X. Chen, 3D mesh labeling via deep convolutional neural networks, ACM Trans. Graphics (TOG) 35 (1) (2015) 3.

[14] Y. Tang, Deep learning using linear support vector machines, in: Workshop on Challenges in Representation Learning, ICML, 2013.

[15] H. Qin, X. Li, J. Liang, Y. Peng, C. Zhang, Deepfish: accurate underwater live fish recognition with a deep architecture, Neurocomputing 187 (2016) 49–58.

[16] S. Iyer, S.K. Sinha, M.K. Pedrick, B.R. Tittmann, Evaluation of ultrasonic inspection and imaging systems for concrete pipes, Autom. Construct. 22 (2012) 149–164.

[17] G. Hinton, L. Deng, D. Yu, G.E. Dahl, A.-r. Mohamed, N. Jaitly, A. Senior, V. Vanhoucke, P. Nguyen, T.N. Sainath, et al., Deep neural networks for acoustic modeling in speech recognition: the shared views of four research groups, IEEE Signal Process. Mag. 29 (6) (2012) 82–97.

[18] Z. Huang, S.M. Siniscalchi, C.-H. Lee, A unified approach to transfer learning of deep neural networks with applications to speaker adaptation in automatic speech recognition, Neurocomputing 218 (2016) 448–459.

[19] P. Sermanet, K. Kavukcuoglu, S. Chintala, Y. LeCun, Pedestrian detection with unsupervised multi-stage feature learning, in: Proceedings of the IEEE Conference on Computer Vision and Pattern Recognition, 2013, pp. 3626–3633.

[20] J. Yu, Y. Rui, Y.Y. Tang, D. Tao, High-order distance-based multiview stochastic learning in image classification, IEEE Trans. Cybern. 44 (12) (2014) 2431–2442.

[21] J. Yu, Z. Kuang, B. Zhang, D. Lin, J. Fan, Image privacy protection by identifying sensitive objects via deep multi-task learning, IEEE Trans. Inf. Forensics Security (2016), doi:10.1109/TIFS.2016.2636090.

[22] Y. Guo, Y. Liu, A. Oerlemans, S. Lao, S. Wu, M.S. Lew, Deep learning for visual understanding: a review, Neurocomputing 187 (2016) 27–48.

[23] C. Hong, J. Yu, J. Wan, D. Tao, M. Wang, Multimodal deep autoencoder for human pose recovery, IEEE Trans. Image Process. 24 (12) (2015) 5659–5670.

[24] C. Hong, X. Chen, X. Wang, C. Tang, Hypergraph regularized autoencoder for image-based 3D human pose recovery, Signal Process. 124 (2016) 132–140.

[25] J. Yu, X. Yang, F. Gao, D. Tao, Deep multimodal distance metric learning using click constraints for image ranking., IEEE Trans. Cybern. PP (2016) 1–11.

[26] Z. İşcan, M.N. Kurnaz, Z. Dokur, T. Ölmez, Ultrasound image segmentation by using wavelet transform and self organizing neural network, Neural Inf. Process. Lett. Rev. 10 (8–9) (2006) 183–191.

[27] A. Ghods, H.-H. Lee, Probabilistic frequency-domain discrete wavelet transform for better detection of bearing faults in induction motors, Neurocomputing 188 (2015) 206–216.

[28] G.G. Yen, K.-C. Lin, Wavelet packet feature extraction for vibration monitoring, IEEE Trans. Ind. Electron. 47 (3) (2000) 650–667.

[29] E. Ortiz, V. Syrmos, Support vector machines and wavelet packet analysis for fault detection and identification, in: International Joint Conference on Neural Networks, 2006, pp. 3449–3456.

[30] J. Qu, Z. Zhang, T. Gong, A novel intelligent method for mechanical fault diagnosis based on dual-tree complex wavelet packet transform and multiple classifier fusion, Neurocomputing 171 (2016) 837–853.

[31] D.K. Hsu, Nondestructive inspection of composite structures: methods and practice, in: 17th World Conf. Nondestruct. Test., 2008, pp. 25–28.

[32] T. Hasiotis, E. Badogiannis, N.G. Tsouvalis, Application of ultrasonic c-scan techniques for tracing defects in laminated composite materials, Strojniški vestnik—J. Mech. Eng. 57 (3) (2011) 192–203.

[33] J.-D. Wu, C.-H. Liu, An expert system for fault diagnosis in internal combustion engines using wavelet packet transform and neural network, Expert Syst. Appl. 36 (3) (2009) 4278–4286.

Min Meng received her Ph.D. degree in Applied Mathematics from Zhejiang University in 2011. She is currently an associate professor at Department of Computer Science, Guangdong University of Technology, China. Her research interests include geometry processing, computer graphics, visual computing and machine learning.

Yiting Jacqueline Chua joined School of Mechanical and Aeronautical Engineering as a research engineer. She graduated with a Diploma in Chemical Process Technology in 2011 and an Advanced Diploma in Polymer Technology in 2013.

Erwin Wouterson received his Ph.D. in Materials Science and Engineering from the Nanyang Technological University in 2008. He is currently a senior lecturer in the School of Mechanical and Aeronautical Engineering of Singapore Polytechnic. His research interests include carbon and glass fiber-reinforced composites, polymer foams, and polymer coatings.

Kelvin Ong received his B.Eng. and M.Sc. from the University of Salford, UK in 1997 and 1999 respectively. He is currently a senior lecturer in the School of Mechanical and Aeronautical Engineering of Singapore Polytechnic. His research interest includes developing applied composites engineering.